Phosphorus speciation in cultivated organic soils revealed by P K-edge XANES spectroscopy

Frank Schmieder[1]*, Jon Petter Gustafsson[1,2], Wantana Klysubun[3], Franz Zehetner[4], Matthew Riddle[1], Holger Kirchmann[1], and **Lars Bergström[1]**

[1] Department of Soil and Environment, Swedish University of Agricultural Sciences, P.O. Box 7014, SE-75007 Uppsala, Sweden
[2] Division of Land and Water Resources Engineering, KTH Royal Institute of Technology, Teknikringen 76, 100 44 Stockholm, Sweden
[3] Synchrotron Light Research Institute (SLRI), 111 University Avenue, Muang District, Nakhon Ratchasima 30000, Thailand
[4] Department of Forest and Soil Science, Institute of Soil Research, University of Natural Resources and Life Sciences, Peter-Jordan-Straße 82, 1190 Vienna, Austria

Abstract

Cultivated organic soils make a significant contribution to phosphorus (P) leaching losses from agricultural land, despite occupying a small proportion of cultivated area. However, less is known about P mobilisation processes and the P forms present in peat soils compared with mineral soils. In this study, P forms and their distribution with depth were investigated in two cultivated Histosol profiles, using a combination of wet chemical extraction and P K-edge X-ray absorption near-edge structure (XANES) spectroscopy.

Both profiles had elevated P content in the topsoil, amounting to around 40 mmol kg^{-1}, and P speciation in both profiles was strongly dominated by organic P. Topsoils were particularly rich in organic P (P-org), with relative proportions of up to 80%. Inorganic P in the profiles was almost exclusively adsorbed to surface reactive aluminium (Al) and iron (Fe) minerals. In one of the profiles, small contributions of Ca-phosphates were detected.

A commonly used P saturation index (PSI) based on ammonium-oxalate extraction indicated a low to moderate risk of P leaching from both profiles. However, the capacity of soil Al and Fe to retain P in organic soils could be reduced by high competition from organic compounds for sorption sites. This is not directly accounted for in PSI and similar indices.

Accumulation of P-org in the topsoil may be attributable by microbial peat decomposition and transformation of mineral fertiliser P by both microbiota and crops. Moreover, high carbon–phosphorus ratio in the surface peat material in both profiles suggests reduced net mineralisation of P-org in the two soils. However, advancing microbial peat decomposition will eventually lead to complete loss of peat horizons and to mineralisation of P-org. Hence, P-org in both profiles represents a huge potentially mobilised P pool.

Key words: Histosol / organic phosphorus / phosphorus saturation / soil aluminium / soil iron / X-ray absorption spectroscopy

Accepted March 19, 2020

1 Introduction

Drainage and agricultural use of peatlands is increasing world-wide (*Oleszczuk* et al., 2008). While profitable, cultivation of organic soil for crop production can have several negative environmental effects. Soil subsidence, ultimately leading to loss of soil, and emissions of greenhouse gases are two examples (*Oleszczuk* et al., 2008; *Berglund* and *Berglund*, 2010; *Knox* et al., 2015). Another significant environmental concern is export of phosphorus (P) from cultivated Histosols. Phosphorus losses play a key role in eutrophication of surface waters (*Schindler*, 1977).

Up to 30 kg P per hectare can annually be leached from cultivated Histosols (*Duxbury* and *Peverly*, 1978; *Miller*, 1979). Losses of this magnitude can contribute significantly to overall P export from arable land, despite a low proportion of peat soils in total arable land area (*Oleszczuk* et al., 2008). For instance, according to *Longabucco* and *Rafferty* (1989), P losses from cultivated Histosols account for an estimated 86% of the total annual P load from a watershed in New York State (USA), even though cultivated Histosols represent only 27% of arable land in the watershed. In Sweden, Histosols occupy 10% of the total area of cultivated land. The annual P losses from mineral soils in Sweden rarely exceed 2 kg ha^{-1} (*Ulén* and *Jakobsson*, 2005; *Berglund* and *Berglund*, 2010).

The development of adequate strategies to minimise P losses from cultivated Histosols requires detailed knowledge of the processes leading to P mobilisation in these soils. However, advances in understanding these processes have been hampered, partly because analytical P speciation in organic soils

* Correspondence: F. Schmieder; e-mail: frank.schmieder@slu.se

is methodologically challenging (*Kruse* and *Leinweber*, 2008). Histosols are naturally rich in organic P and this P fraction has been the focus of many previous studies, in which liquid-state ^{31}P nuclear magnetic resonance (NMR) spectroscopy has been applied (*Bedrock* et al., 1994; *Robinson* et al., 1998; *Li* et al., 2013). *Robinson* et al. (1998) found monoester phosphate to be the dominant P species in NaOH-EDTA extracts of Histosols. *Bedrock* et al. (1994) identified among other phosphonates and pyrophosphate in Histosols.

However, P in leachate from cultivated Histosols has primarily been found to be inorganic (*Duxbury* and *Peverly*, 1978; *Miller*, 1979; *Reddy*, 1983). Moreover, leaching losses have been related to fertilisation rates and content of Fe and Al mineral phases (*Miller*, 1979). Hence, knowledge of binding forms of mineral P may be crucial in understanding P leaching from cultivated Histosols (*Miller*, 1979). This includes the environmentally problematic increases in soil solution P frequently observed in recently restored cultivated wetlands (*Jensen* et al., 1998; *Zak* and *Gelbrecht*, 2007). Phosphorus mobilisation from restored wetlands has frequently been attributed to reductive dissolution of Fe^{3+}-(hydr)oxide minerals, whereby adsorbed P is released after cessation of drainage (*Jensen* et al., 1998; *Zak* and *Gelbrecht*, 2007; *Emsens* et al., 2016).

Many previous studies on characterisation of mineral P in Histosols have relied on chemical fractionation schemes (*e.g.*, *Hedley* et al., 1982; *Robinson* et al., 1998; *McCray* et al., 2012). However, these merely describe the distribution of P into operationally defined fractions, leaving uncertainty as regards the real chemical nature of P in soils (*Condron* and *Newman*, 2011). In addition, application of extraction schemes to Histosols tends to result in high proportions of poorly defined residue P (*Schlichting*, 2004; *Kruse* and *Leinweber*, 2008). It would therefore be preferable to study P speciation in Histosols using more direct approaches, such as P K-edge X-ray absorption near-edge structure (XANES) spectroscopy (*Hesterberg* et al., 1999). This technique allows direct identification of P species in soils without the need for an extraction step that could potentially alter the chemical state of P in the sample (*Kizewski* et al., 2011). Identification of P species and relative quantification in a mixed sample such as soil can be done using least square fitting approaches (*e.g.*, linear combination fitting, LCF). It is thereby crucially important that the XANES spectra of P species contained in a sample have unique spectral features that allow identification (*Hesterberg*, 2010). Examples are the pre-edge feature typical for Fe^{3+}-associated P and the post-edge shoulder in calcium phosphate spectra (*Hesterberg*, 2010). Organic P species are in turn often considered problematic as their XANES spectra usually lack unique and distinguishable spectral features (*Kruse* and *Leinweber*, 2008). Phosphorus *L*-edge XANES could be an alternative to circumvent this problem since *L*-edge spectra of organic compounds tend to feature more specifically distinguishable characteristic (*Kruse* et al., 2015). However one important limitation regarding P *L*-edge XANES is the high P concentration of at least 5 to 10 g P kg^{-1}, which substantially exceeds P concentration in most pristine and agricultural soils (*Kruse* et al., 2015).

Some P K-edge XANES studies have been conducted on Histosols and organic soil layers (*Kruse* and *Leinweber*, 2008; *Prietzel* et al., 2010). For example, *Kruse* and *Leinweber* (2008) collected XANES spectra from the residues after each fractionation step and concluded from their data that the Hedley scheme may not be sufficiently selective in organic soils. Changes in the spectra often did not reflect removal of P species targeted with a specific extraction step. Based on LCF results, *Prietzel* et al. (2010) found organic layers in forest soil to be dominated by inorganic P.

Thus, P K-edge XANES spectroscopy can provide valuable information on P speciation in Histosols and thereby help to reduce the uncertainty in results obtained with chemical fractionation methods. The aim of this study was thus to characterise P in cultivated Histosol profiles. An extensive library of reference spectra of both organic and inorganic P species was used in LCF analysis to obtain information on the P speciation in these soils. Moreover, a thorough characterisation of relevant physical and chemical properties of the soil profiles was made, to complement the XANES results. Both topsoil and subsoil layers were studied to account for the potential importance of subsoil properties on P leaching losses to drainage systems (*Andersson* et al., 2013).

2 Material and methods

2.1 Soil sampling and characterisation

Two cultivated organic fen-peat soils were sampled, both located near Lake Hjälmaren in Örebro County, Sweden. Both soil profiles were classified as Typic Haplosaprists (USDA-NRCS classification) and both had a layer of underlying mineral soil at 90–100 cm depth, which was included in sampling. One of the sample sites, both being commercially cultivated, hereafter referred to as H1, had received mineral P fertiliser at a rate of approximately 20 kg ha^{-1} y^{-1} for the previous nine years. The other soil (H2) had received, on average, annual P fertiliser at a rate of 18 kg ha^{-1} y^{-1} for the previous 10 years. Commonly cultivated crops on H1 were spring wheat (*Triticum aestivum* L.), spring barley (*Hordeum vulgare* L.), and potatoes (*Solanum tuberosum* L.). Crops grown on H2 included wheat, potatoes, and carrots (*Daucus carota* L.). Tile drains were installed in both soils to about 80–100 cm depth back in the 1940s.

In both profiles, soil samples were taken from the top layer (20 cm depth), which was homogeneous due to soil tillage. Below this layer, sampling was carried out at 10 cm intervals down to 100 cm in the case of H1 and 90 cm in the case of H2, including samples of the mineral layers underlying the organic material in both cases. All soil samples were air-dried, homogenised, and stored at 5°C until further analysis. Particle size distribution was determined according to *ISO 11277* (2009). This included removal of organic material with heated hydrogen peroxide. The pH of dried samples was determined in deionised water at a ratio (w/v) of 1:5. Total carbon (C-tot) and nitrogen (N-tot) were determined using a Leco Tru-Mac analyser (LECO, St. Joseph, MI) following *ISO 13878* (1998).

2.2 Wet chemical analyses

Acid digestion of soil samples before element analysis was carried out with concentrated HNO_3 at three temperature stages (60°C to 130°C) over 5 h according to a modified *ISO 11885* (2007) standard. Concentrations in the digestate of Fe (Fe-pstot), Al (Al-pstot), calcium (Ca-pstot), and P (P-pstot) were determined using inductively coupled plasma atomic emission spectroscopy [ICP-OES (Optima 7300 DV, PerkinElmer, MA, USA)], where the term (-pstot) refers to "pseudo-total" following international standards (*ISO 11074*, 2015), as the acid digestion procedure may not be strong enough to completely recover the total element content from a sample. A wet-chemical estimate of organic P was obtained according the Ignition method (*Kuo*, 1996).

Surface-reactive, poorly crystalline Fe and Al and associated P (Fe-ox, Al-ox, and P-ox) was estimated by extraction with 0.2 M ammonium oxalate-oxalic acid (pH 3), carried out in darkness for 4 h at a soil:solution ratio of 1:100 according to *Schwertmann* (1964). Phosphorus saturation index (PSI), a widely used empirical index for P leaching risk assessment, was then calculated as (*Lookman* et al., 1995):

$$PSI = \frac{P\text{-}ox}{0.5\times(Fe\text{-}ox + Al\text{-}ox)}. \quad (1)$$

To obtain an estimate of Fe and Al associated with organic matter in the two soils, pyrophosphate extraction (Fe-pyr, Al-pyr) was carried out according to *McKeague* (1967). Samples were suspended in 0.1 M sodium pyrophosphate at a soil:solution ratio of 1:100 and extracted for 16 h. The extract solution was subsequently filtered through general-purpose filter paper. Citrate-dithionite extraction (Fe-dith, Al-dith), a representation of more crystalline forms of Fe and Al, was carried out following *Holmgren* (1967). A suspension containing 2 g of solid sodium dithionite, 1 g sample soil and 100 mL of a sodium citrate/sodium bicarbonate solution was shaken for 16 h. The concentrations of Al and Fe in the extract were determined using ICP-OES as described above.

2.3 P K-edge XANES analysis

Both sample and standard P K-edge XANES spectra were collected at beamline 8 of the Synchrotron Light Research Institute (SLRI) in Nakhon Ratchasima, Thailand (*Klysubun* et al., 2012). At the facility, a 1.3 GeV beam storage ring with a beam current of 80–150 mA was used. The beamline was equipped with an InSb(111) double crystal monochromator, resulting in a 17.7 × 0.9 mm^2 beam with a flux of 1.3 × 109 to 6 × 1010 photons s^{-1} (100 mA)$^{-1}$. Measurements were carried out in fluorescence mode.

Sample preparation included air-drying, milling and sieving to obtain a maximum particle size of 0.05 mm. A thin layer of sample material was applied onto P-free Kapton tape in a sample holder, which was sealed on the upper side with polypropylene X-ray film. Before the experiments, it was ascertained that none of the materials used for sample preparation was contaminated with P. The sample compartment was filled with helium (He) gas. The intensity of the incoming beam was determined with a N_2 gas-filled ion chamber. Fluorescence measurements were carried out with a solid-state 13-element Ge detector. The measured fluorescence energy interval was 2100–2320 eV. The energy steps were smallest (0.2 eV) close to the absorption edge (E_0) between 2140 and 2155 eV. In other energy ranges, the energy steps were up to 0.5 eV. The number of scans varied between 3 and 10, depending on the sample P concentration.

Prior to the experiment, the beam energy was calibrated by setting the maximum of the first derivative of the spectrum (E_0) for elemental P powder (red phosphorus) to 2145.5 eV. In addition, XANES spectra of a variscite standard sample (E_0 = 2154.05 eV) were regularly collected during the beam sessions. This was done to detect unwanted energy shifts. Energy differences between E_0 observed for the variscite spectra were used to correct E_0 in sample spectra collected around the same time (*Eriksson* et al., 2016). These energy corrections and all other data processing were carried out with the Athena software package version 0.9.024 (*Ravel* and *Newville*, 2005). This included energy calibration, merging/normalisation of sample scans and LCF analysis. Care was taken to keep the normalisation of sample and reference spectra as consistent as possible. In a few cases, however, the normalisation energy range had to be slightly adjusted to deal with inconsistencies in baseline and background trends. Generally, baseline correction was done by subtracting a linear function from the pre-edge region at –30 eV to –10 eV relative to E_0 from the spectra. The edge step used for the normalisation was determined with a linear function across the post-edge region between 30 eV and 45 eV relative to E_0.

Linear combination fitting to determine the P speciation in samples followed a procedure from *Tannazi* and *Bunker* (2005). The reference library used for LCF was established and used previously by *Eriksson* et al. (2016). Included were organic P compounds, Fe, Ca and Al phosphate minerals, and phosphate adsorbed on Fe and Al (hydr)oxides (Fig.1). All reference spectra were collected at the same beamline. Merged sample scans were fitted with the complete library of reference spectra. However, a maximum of only four references was allowed in the final fits to avoid overfitting. Fitting was carried out over an energy range of 2144 eV to +2184 eV, *i.e.*, from –10 to 30 eV relative to the E_0 of variscite.

A precondition for the LCF fits to be acceptable was that the sum of the relative proportions of the references included in the fits was within the range 90–110%. Accepted fits were then re-normalised to match a summed proportion of 100%. The ranking of the accepted fits was based on the R factor (*Ravel* and *Newville*, 2005; *Ravel*, 2009), as an indicator of the goodness-of-fit.

3 Results

3.1 Wet chemical analyses

The organic horizon in profiles H1 and H2 was 90 and 80 cm thick, respectively. Physical and chemical properties, including those for the underlying mineral soil layers, are presented

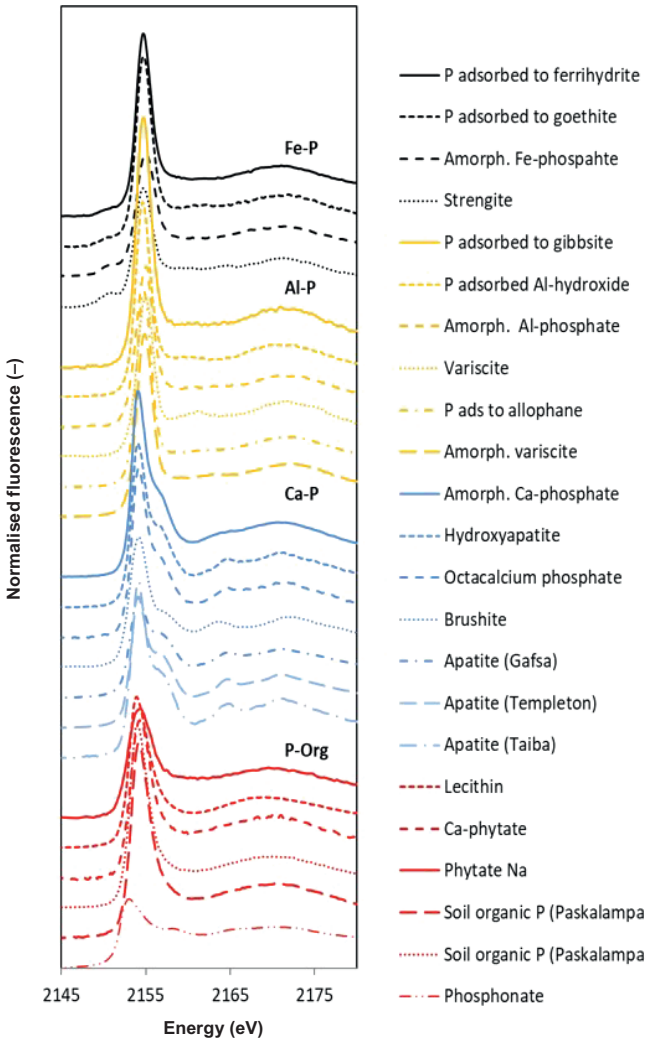

Figure 1: Normalised reference phosphorus K-edge X-ray absorption near-edge structure (P K-edge XANES) spectra used in linear combination fitting (LCF).

in Tab. 1. The soil pH in both profiles was acidic, ranging between 4 and 6. The profiles were free of inorganic carbonate. Organic C content (C-org) and total N contend (TOT-N) tended to decrease with soil depth in the two profiles. The nutrient ratios C:N and C:P were in turn higher in the organic subsoil layers of both profiles in comparison to upper soil layers.

Common in both profiles was a clear enrichment with Fe-pstot in the organic sub soil layers directly overlying the mineral soil layers. With 726 mmol kg^{-1} and 696 mmol kg^{-1} in H1 and H2, respectively, the Fe-pstot content in these layers exceeded the content in the remainder of the profiles at least by a factor of 2 (Tab. 2).

The extractability of Fe with ammonium-oxalate (Fe-ox) relative to Fe-pstot content was highest in the top soil of both profiles. Up to 90% and 60%-of top soil Fe-pstot, was ammonium-oxalate extractable in H1 and H2, respectively. The corresponding top soil Fe-ox content in H2 (70 mmol kg^{-1}) was nevertheless lower than in the sub soil, while Fe-ox content throughout most of the H1 profile ranged around 120 mmol kg^{-1}.

Dithionite-extractable Fe followed a vertical pattern similar to the Fe-ox content in both profiles. The content of both was very similar as well; with Fe-dith tending to be slightly lower (Tab. 2).The results of pyrophosphate extraction suggested that a considerable proportion of Fe in both profiles was associated with organic matter. Relative to the corresponding Fe-pstot content, recovery as pyrophosphate extractable Fe (Fe-pyr) was high in the topsoil of both profiles, corresponding to a Fe-pyr content of 102 mmol kg^{-1} in H1(60%) and 55 mmol kg^{-1} in H2 (36%).

In both profiles, Al-pstot content was lowest in the upper 20 cm. In the H2 profile, the content increased from around 150 mmol kg^{-1} to a maximum of 660 mmol kg^{-1} at 60–70 cm soil depth. In H1, the highest content (> 1000 mmol kg^{-1}) was observed in the 30–50 cm soil layer with its elevated ash and clay content.

The method for determination of the particle size distribution had primarily been developed for mineral soils and it proofed difficult to yield enough mineral material for analysis from the peat samples. Nevertheless clay content was strongly and significantly correlated with AL-pstot in the H1 profile (R^2 = 0.92; p < 0.0005). Content of Al-ox in the profiles followed the vertical pattern seen for Al-pstot, but the relative recovery of Al-ox decreased with depth. The highest content in the H1 soil (up to 415 mmol kg^{-1}) was found at 30–60 cm depth. The content of Al-ox in soil H2 was considerably lower and did not exceed 122 mmol kg^{-1} (40–50 cm later). Similarly, to Fe-dith, the Al-dith content was consistently lower than the Al-ox content. A considerable proportion of Al-pstot in the two profiles was extractable with pyrophosphate as well.

The pseudo-total P content was clearly elevated in the topsoils of both profiles and ranged between 30 and 45 mmol kg^{-1}, with slightly higher contents observed in H2. In the subsoil of both profiles, P-pstot content remained below 20 mmol kg^{-1}. It was found that the P-pstot content of the high ash content layers at 30–60 cm depth H1 were entirely extractable with oxalate, to a maximum of 31 mmol kg^{-1}. Recovery of P-ox relative to P-pstot was otherwise lower, amounting to 50% P-pstot in the top 20 cm and declining to around 30% in the subsoil. In the H2 profile, relative recovery was less variable and remained at around 40%, which corresponded to a P-ox content decreasing from a maximum of 19 mmol kg^{-1} in the topsoil to 7.5 mmol kg^{-1} in the subsoil. In the mineral layers of both profiles, around 80% of P-pstot was ammonium-oxalate extractable.

Mean P-ox content was similar in the two profiles (13.4 and 12.6 mmol kg^{-1} in H1 and H2, respectively). However, due to the higher content of Al-ox in H1, the PSI values were consistently lower in this profile, with a maximum of 0.17 in the topsoil in comparison with 0.29 in H2.

Organic P content in H1, determined according to the ignition method, ranged between 7 and 12 mmol kg^{-1}. In the upper 40 cm, this corresponded to relative proportion of P-org lost

Table 1: Selected physical and chemical properties of the two Histosol soil profiles, H1 and H2.

Profile	Soil layer	pH[a]	Clay[ad]	Silt[ad]	C-org[ab]	Loss on ignition[a]	Tot-N[ab]	C:N[ab]	C:P[ac]
	(cm)	(–)	(%)					(–)	
Histosol 1	0–20	5.3	3.9	11.0	49.3	84.2	3.1	16	1077
	20–30	5.7	7.3	11.4	48.0	80.7	2.9	17	1061
	30–40	6.0	27.5	16.4	33.9	53.7	1.8	19	844
	40–50	5.9	31.4	21.7	27.6	44.3	1.4	20	1127
	50- 60	5.6	20.1	17.7	36.2	57.1	1.5	23	1873
	60–70	5.3	8.1	7.2	48.8	80.7	2.1	23	2259
	70–80	4.5	16.0	19.7	35.5	61.4	1.8	20	1960
	80–90	4.3	18.3	22.9	34.1	56.2	1.7	20	1834
	90–100	4.1	48.4	47.4	1.8	0.6	0.2	10	100
Histosol 2	0–20	5.1	3.5	11.8	45.8	81.2	3.3	14	875
	20–30	5.3	12.4	14.9	40.4	67.7	2.9	14	1034
	30–40	5.5	23.6	19.3	31.4	53.5	2.4	13	803
	40–50	5.7	22.1	20.1	33.5	54.1	1.9	18	1366
	50–60	5.6	25.2	18.6	32.3	52.0	1.8	18	1423
	60–70	5.5	33.2	18.9	26.9	43.8	1.6	17	1382
	70–80	5.4	21.7	20.2	32.1	52.1	1.6	21	1701
	80–90	5.7	49.6	45.5	1.1	0.0	0.1	8	50

[a]Values presented are mean of duplicate samples.
[b]Tot-C = total carbon content (ISO 13878); Tot-N = total nitrogen content (ISO 13878); C:N = ratio of total carbon to total nitrogen.
[c]C/P = ratio of total carbon content and pseudo-total P content (modified ISO 11885:2007).
[d]Clay and silt content are related to bulk soil mass.

on ignition (P-org-ig) of about 30% of P-pstot. This percentage increased to a maximum of 65% in deeper soil layers. In the H2 profile, P-org-ig content tended to be higher, up to 19 mmol kg^{-1} at 20–30 cm depth. As observed for H1, the proportion of organic P relative to P-pstot also increased with soil depth in H2.

3.2 XANES analysis

Figure 2 presents sample spectra collected for the two profiles, including the best fits from the LCF analysis. All collected spectra were of very good quality, with high signal to noise ratio. Sample spectra for the uppermost 20 cm in both soils visibly resembled organic P standard spectra such as lecithin. This resemblance included a shift of the absorption edge position (E_0) towards lower energy in comparison with E_0 of the variscite standard used for the energy calibration (2154.05 eV) and other mineral P reference spectra. Figure 3 illustrates this for the example of the H1 spectrum at 0–20 cm, comparing the edge position (E_0) of this sample at 2153.2 with that of relevant reference spectra. Edge energy positions of sample spectra of the two profiles and selected reference spectra are also presented Tab. 3. In general, E_0 of all sample spectra was lower than in relevant reference spectra for mineral P. However, the lowest E_0 values were observed in sample spectra for the top 20 cm of both profiles.

Despite a generally very high fitting quality in LCF analysis, visual comparison revealed an obvious mismatch between sample and fitted spectra in the post-edge region for some sample spectra of the H1 and H2 profiles. This is shown for the example of the H1 sample spectrum at 30–40 cm soil depth in Fig. 4a, b. Sample spectra that were affected by this were particularly those collected for subsoil layers with relatively elevated extractable Al and ash content. These spectra featured a visible indication of mineral P presence in the post-edge region. As illustrated in Fig. 4b, the fitted spectrum did not adequately represent the 'trough' between absorption edge and the post-edge peak in an energy range between approximately 2158 eV and 2163 eV. Reflecting a P-org weight of 64%, the post-edge region of the fitted spectrum resembled more closely the sample spectrum for the top 20 cm. *Eveborn* et al. (2009) complemented LCF analysis by specifically fitting the sample spectra in the pre-edge region in order to increase the sensitivity for Fe-associated P. In a similar approach, LCF was carried out over the post-edge region from approximately +1 eV to +30 eV relative to E0 for the H1

Table 2: Results of wet chemical analysis of the two Histosol profiles, H1 and H2.

Soill	Layer (cm)	Ca-pstot[a] (mmol kg^{-1})	Fe-pstot[a]	Fe-ox[ab]	Fe-pyr[a]	Fe-dith[a]	Al-pstot[a]	Al-ox[ab]	Al-pyr[a]	Al-dith[a]	P-pstot[a]	P-ox[ab]	P-org_ig[ab]	PSI (%)
H1	0–20	804.8	133.3	115.5	79.4	102.9	138.2	70.6	51.5	58.7	38.1	15.9	7.9	17
	20–30	1046.3	138	125.3	91	118.7	368	282.2	189.3	225.7	37.7	19.7	9.4	10
	30–40	517.8	124.6	71	44.8	66.8	974.3	415.7	281.7	318.9	33.4	31.4	9.3	13
	40–50	399.5	159.8	60.4	37.6	57.2	1131.2	410	269	285.5	20.4	22.5	12.4	10
	50–60	429.1	194.5	114.8	75.4	115.9	809.2	333.9	227.1	251.7	16.1	5.5	10.4	2
	60–70	455.1	258.2	128.6	81.6	127.1	507.1	277.9	200.1	222.6	18	5.9	9.7	3
	70–80	267.9	274	128.3	71.8	126	516.1	181.9	119.6	124.4	15.1	4.4	7.8	3
	80–90	258.7	726	115.9	53.7	110.4	548.4	164.2	108.7	114.7	15.5	4.4	6.6	3
	90–100 (mineral)	183.1	168.6	90.7	24.5	77.7	1151.5	65.8	3.4	17.1	14.9	12.7	0.7	16
H2	0–20	587.2	102.9	67.1	36.8	57.5	152.1	69.8	54	54.6	43.6	18.2	13.6	27
	20–30	396.1	173.6	39.8	16	34.7	174.6	61	35.6	43	32.5	11.1	19.8	22
	30–40	370.6	320.8	57.2	22.9	51.5	344.4	84.2	42.7	58.3	32.6	14.3	18.7	20
	40–50	469.3	334.4	117.3	42.6	103.7	520.6	122.2	63.6	76.4	20.4	9.4	16	8
	50–60	406.1	366	113.7	46.1	101.5	552	118.1	55.7	66.2	18.9	8.2	15.6	7
	60–70	320.6	337	nd	nd	nd	656.6	nd	nd	nd	16.2	nd	12.7	nd
	70–80	366.5	695.5	102.4	33.9	88.8	514.8	98	45.1	48.8	15.7	7.5	11.5	7
	80–90 (mineral)	157.1	124.9	53.3	9.8	29.1	1149.5	63.3	1.6	9.3	17.6	13.2	9.1	23

[a]Values presented are means of duplicate samples.
[b]pstot = pseudo-total, extractable with concentrated HNO_3;, -ox = ammonium oxalate extractable, -pyr = pyrophosphate extractable, -dith = dithionite extractable.
PSI = Phosphorus saturation index.

and H2 sample spectra. The composition of these fits differed from those carried out over the whole XANES energy region. The major difference was a reduced contribution of P-org references in favour of an increased weight of phosphate adsorbed to Fe/Al mineral phases. For instance, the P-org weight in the post-edge fit for the H1 sample at 30–40 cm depth decreased from 64% to 23%. As can be seen in Fig. 4b, post-edge fits resembled the sample spectra in the post-edge region considerably more than the original fit over the complete XANES energy region. However, this came at the cost of a poorly fitted absorption edge in comparison with the sample spectrum (Fig. 4c).

Nevertheless, post-edge fitting results regarding adsorbed mineral P for H1 were overall better correlated with extractable Fe, Al, and P content. For instance, R^2 for the correlation between pooled weights of Fe–P and AL-P and Al-pstot content increased from 0.7 to 0.9 ($p < 0.0005$). Moreover, an improved correlation ($R^2 = 0.8$; $p < 0.005$) with Al-ox content was observed. A slight improvement in the correlation between the calculated content of adsorbed P and P-ox was achieved when using post-edge LCF results, with R2 increasing from 0.8 to 0.9 ($p < 0.0005$). For the H2 profile, a similar improvement in correlation between LCF results and results of wet chemical analyses was not observed. However, for this profile, differences between original and post-edge LCF results were less pronounced.

A pre-edge shoulder situated at around 2149 to 2152 eV, indicative of Fe-associated P (*Hesterberg* et al., 1999), was not visible in the spectra. The spectra collected for the mineral soil layer in both profiles featured a shoulder at around 2157.5 eV. Additionally, two post-edge peaks at 2164.7 eV and 2171.3 eV were present which in combination with the pre-edge shoulder indicated the presence of calcium phosphates (*Zuo* et al., 2015). Values of the goodness-of-fit factor R from the LCF analysis were in the lower range of those reported in previous studies (*Eveborn* et al., 2014; *Eriksson* et al., 2016) (Tab. 4). The weights listed refer to the best fits, *i.e.*, those to which the lowest R-value was assigned. Reference spectra included in the best fits were categorized into groups, whose relative contribution to the final fits are shown in Tab. 4. The number of occurrences (count) of representatives of a specific P group in the 10 best fits is also presented in the table. Generally, the fitting quality did not decline substantially within the 10 best fits for a particular sample spectrum. Moreover, the relative contribution of P groups remained similar within the 10 best fits.

Results from LCF generally reflected the presence of P species that were visually observable in the sample spectra. The dominant P form in both profiles according to LCF was P-org, which at most comprised around 80% in the top 20 cm of both profiles. In deeper organic layers of H1, P-org weight decreased to 60%. In the H2 soil, the lowest P-org weights (50%) were observed in fits for two subsoil layers that included references for calcium phosphates. The latter were otherwise absent in organic layers of H1 and H2. Corresponding weights of Ca–P in these fits amounted at most to 17%. Expectedly, the mineral soil underlying both profiles contained substantially less P-org, with LCF weights of less than 13%.

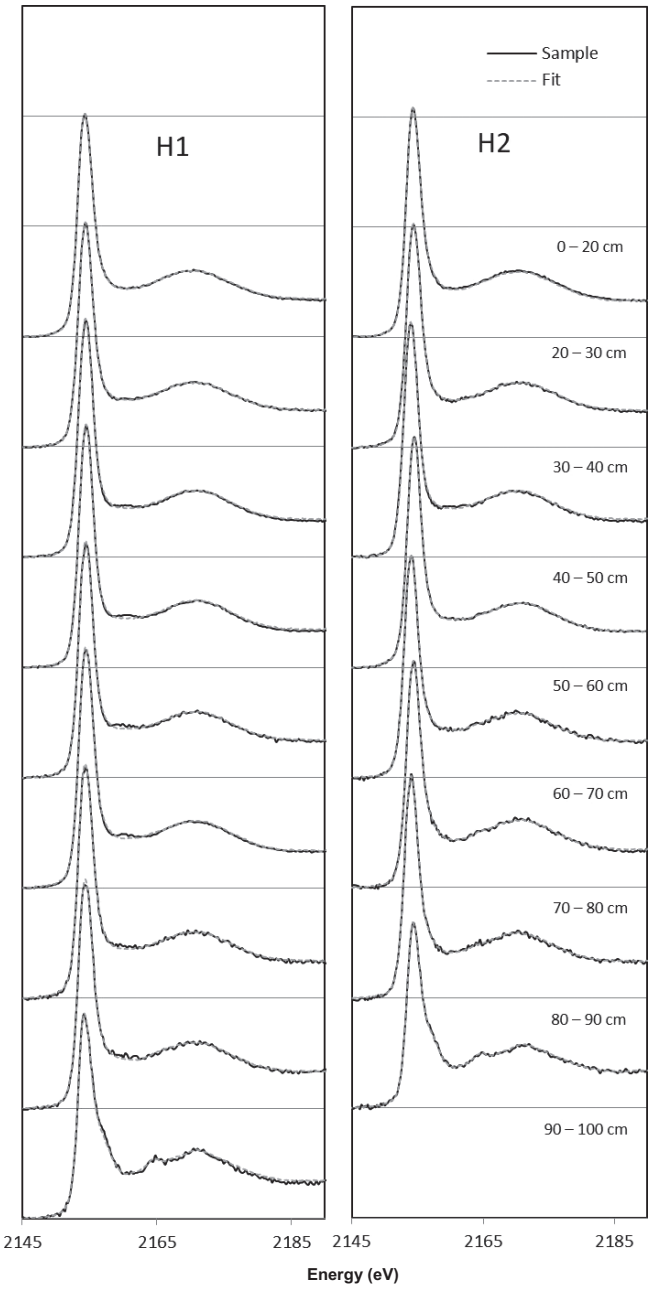

Figure 2: Phosphorus (P) K-edge X-ray absorption near-edge structure (XANES) sample spectra and best fita from linear combination fitting for Histosol profile (left) H1 and (right) H2. ”a” assigned the lowest R factor (*Ravel* and *Newville*, 2005).

Apart from the mentioned occurrences of Ca–P, inorganic P references included in LCF fits for the organic layers almost exclusively represented P adsorbed to Al and Fe mineral surfaces, particularly reference spectra for phosphate adsorbed to gibbsite (Al–P) and goethite (Fe–P).

In the H1 soil, the weight of Al-bound P reached a maximum of 35% in the 40–50 cm layer. Below this depth Al–P contribution declined to about 6% at 80–90 cm. Topsoil Al–P contribution did not exceed 10%. According to the LCF results, Fe–P was concentrated in the subsoil of the H1 profile, contributing

Table 3: Absorption edge position (E_0) for phosphorus K-edge X-ray absorption near-edge structure (P K-edge XANES) sample spectra for the Histosols H1 and H2 and selected reference spectra (defined as the maximum in first derivative of the spectra).

Soil depth	E_0 (eV)		
(cm)	H1	H2	Reference spectra
0–10	2153.2	2153.2	
10–20			
20–30	2153.4	2153.4	
30–40	2153.3	2153.5	
40–50	2153.4	2153.4	
50–60	2153.4	2153.5	
60–70	2153.4	2153.4	
70–80	2153.3	2153.5	
80–90	2153.4	2153.4	
90–100	2153.4		
P adsorbed to ferrihydrite			2153.9
P adsorbed to gibbsite			2153.9
Hydroxyapatite			2153.4
Lecithin			2153

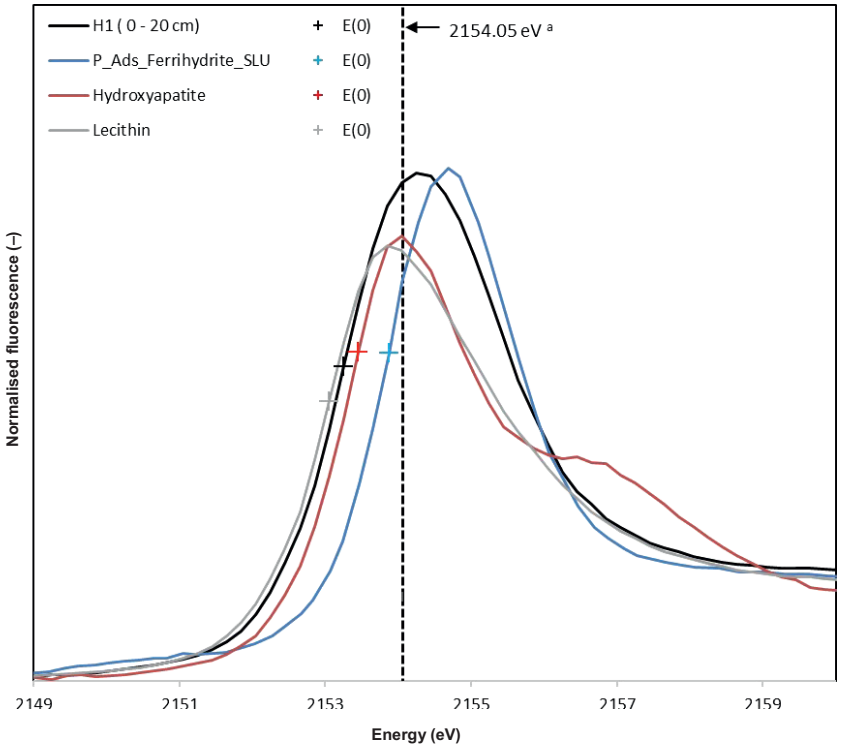

Figure 3: Normalised phosphorus (P) K-edge X-ray absorption near-edge structure (XANES) spectra for the H1 sample from 0–20 cm and reference spectra of P adsorbed to aluminium hydroxide (P_Ads_AlOH3), hydroxyapatite, and lecithin (organic P-diester). Energy positions of the absorption edge (E0), marked in the diagram with "+", are defined as first maximum of the second derivative of the spectra. [a]Energy position of the variscite reference used for the energy calibration of sample and reference spectra.

up to 25% (80–90 cm). In contrast, there was no contribution of Fe–P in best fits for the subsoil layers of H2. Instead, LCF resulted in high Al–P weights in these layers of up to 37% (70–80 cm).

Figure 5 presents P content corresponding to the weights of the P groups in relation to P-pstot content. As can be seen, LCF results corresponded to an increase in P-org content towards the topsoil in both profiles. In the top 20 cm, LCF-based content amounted to as much as 30 mmol kg^{-1} of P-org, exceeding subsoil P-org content by up to threefold. Pooled content of P adsorbed to Fe and Al surfaces also tended to be higher in upper soil layers, but did not exceed 12 mmol kg^{-1}. The weight of Ca–P in the sub soil of H2 corresponded to a content of 2–3 mmol P kg^{-1}. In the mineral soil layers of both profiles, Ca–P was dominant, amounting to 10 mmol kg^{-1} in both.

Results from LCF were significantly correlated with relevant results from the complementary chemical and physical analysis. For instance, in both profiles the pooled LCF weight of inorganic P adsorbed to Fe and Al was significantly correlated with the Al-pstot content (H1: $R^2 = 0.67$, $p < 0.05$; H2: $R^2 = 0.73$; $p < 0.05$). Moreover, Al–P content in the H1 profile, calculated from LCF weight and corresponding P-pstot content, was significantly correlated with P-ox ($R^2 = 0.65$; $p < 0.05$). Pooling Al–P content with Fe–P content led to significant correlations with P-ox in both profiles (H1: $R^2 = 0.82$, $p < 0.05$; H2: $R^2 = 0.7$, $p < 0.05$)

4 Discussion

4.1 Wet chemical analyses

With ash content consistently exceeding 5% in both profiles, soils H1 and H2 can be referred to as minerogenic peat soils (*Tolonen*, 1984; *Steinmann* and *Shotyk*, 1997). Decreasing C:N and C:P ratios indicated a higher degree of decomposition of the topsoil peat material as compared to sub soil layers. Accumulation of nutrients relative to C-org content is commonly observed during organic matter decomposition (*Biester* et al., 2014; *Drzymulska*, 2016).

It may appear contradictory that C-org content in both profiles was highest in the topsoil, as the mineral content is generally expected to increase in topsoil of drained organic soils (*Kasimir-Klemedtsson* et al.,

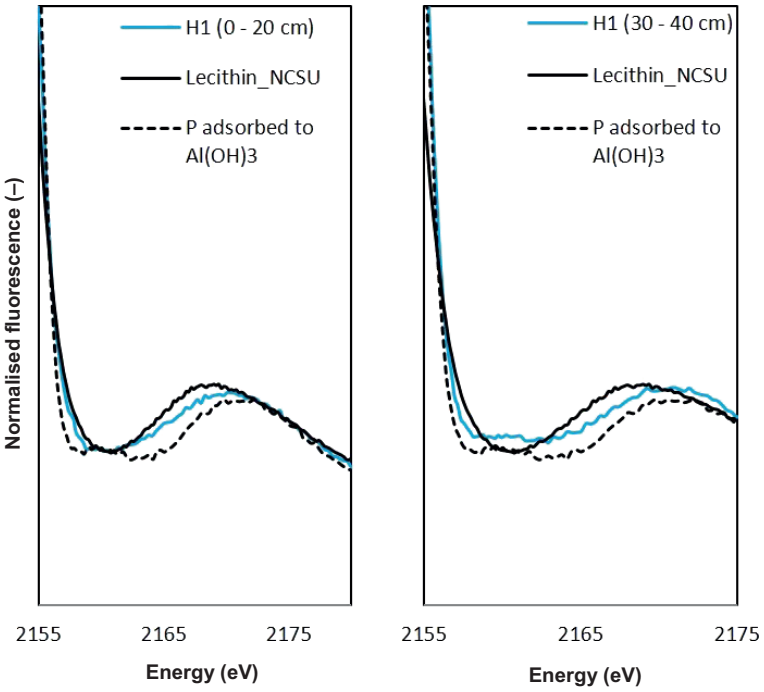

Figure 4: Post-edge oscillation of Histosol profile H1 sample spectra collected at (left) 0–20 cm and (right) 30–40 cm depth in Histosol profile H1, in comparison with reference spectra for lecithin (organic P) and phosphorus (P) adsorbed to amorphous aluminium hydroxide $[Al(OH)_3]_4$.

1997; *Leifeld* et al., 2011). However, temporally and locally varying input of mineral material *via* surface runoff or groundwater flow, which is typical for fens, may overshadow this pattern (*Smieja-Król* and *Fiałkiewicz-Kozieł*, 2014).

Pseudo-total Fe content in both profiles was in the lower range of values reported for fen peats in previous studies (*Zak* et al., 2010). Exceptions to this were the organic layers lying above the mineral soil in both profiles. Similar peaks in soil Fe in peat soils have been reported previously (*Hill* and *Siegel*, 1991; *Steinmann* and *Shotyk*, 1997). *Hill* and *Siegel* (1991) attributed such accumulation of Fe in the mineral soil peat interphase to groundwater discharge and organic complexation of dissolved Fe upon contact with the peat layer.

The similarity between Fe-dith and Fe-ox results in the profiles indicates a low content of crystalline Fe-oxide phases. This may be explained by the relatively short time of 70 years since drainage of the peat, which may have been too short a period for significant formation of crystalline Fe^{3+} minerals (*Stoppe* et al., 2015). Recurring periods of reducing conditions may have further inhibited crystallisation of mineral oxides (*Oenema*, 1990).

In both profiles, the extractability of Fe with oxalate tended to be slightly higher in comparison with Fe-dith. By definition, Fe-ox should be included in the iron pool extracted with dithionite (*Mehra* and *Jackson*, 1960). The differences between Fe-dith and Fe-ox in the profiles were generally low and may reflect uncertainty in the measurements. An excess of Fe-ox content relative to Fe-dith content has been observed in coastal sediments and was attributed to dissolution of magnetite (*Stoppe* et al., 2015). In comparison with the present study, Fe-ox : Fe-dith ratios, observed in *Stoppe* et al. (2015), were, however, with up to 2.2 higher. Generally, determining the specific reason for possible excess Fe-ox in the H1 and H2 profiles was beyond the scope of the present study.

The Al content in the H1 profile can be considered high for an organic soil. For instance, *Schlichting* (2004) found a maximum Al-ox content of 166 mmol kg^{-1} in topsoil samples of different European fen peats, whereas Al-ox amounted to 400 mmol kg^{-1} in H1. The strong correlation of Al-pstot with clay content suggests the particle size distribution was reasonable despite the method used being developed primarily for mineral soils. Moreover, it indicates most Al has been deposited with mineral particles during the formation of the peat profiles.

Pyrophosphate extraction results suggested a high proportion of organically complexed Al and Fe. Considering the high organic matter content in the two profiles, a high percentage of pyrophosphate extractable Fe and Al could be expected,

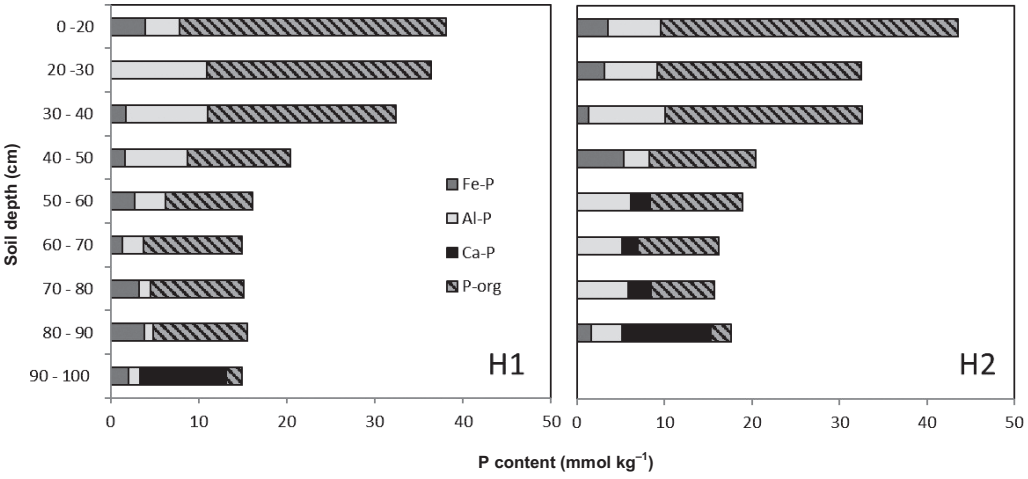

Figure 5: Phosphorus (P) speciation in Histosol profile (left) H1 and (right) H2 according to linear combination fitting (LCF) results. The content was calculated as the product of LCF best fit weights for iron-associated phosphorus (Fe–P), aluminium-associated P (AL–P), calcium phosphates (Ca–P) and organic P (P-org), and corresponding HNO_3 extractable phosphorus (P-pstot) content.

Table 4: Results from linear combination fitting (LCF) for soil layers in Histosol profiles H1 and H2. Phosphorus reference spectra of the 10 best fits are summarised into P groups (P adsorbed to Fe; Fe-phosphates; P adsorbed to Al; Al-phosphates; Ca-phosphates; P-org). The relative contribution of each P group to the best fit (weight %) for a sample spectrum and the number of occurrences of reference spectra representing P groups within the 10 best fits (Count 10BF) are also shown. The best fit in this context refers to the fit with the lowest value of R (*Ravel* and *Newville*, 2005).

	Soil layer	P adsorbed to Fe[a]		Fe-phosphates[a]		P adsorbed to Al[a]		Al-phosphates		Ca-phosphates		P-org[b]		
	(cm)	Weight[a] (%)	Count 10 BF[b]	Weight[a] (%)	Count 10 BF[b]	Weight[a] (%)	Count 10 BF[b]	Weight[a] (%)	Count 10 BF[b]	Weight[a] (%)	Count 10 BF[b]	Weight[a] (%)	Count 10 BF[b]	*R*[c]
H1	0–20	10 ± 1	2	0	0	10 ± 0	10	0	0	0	3	79 ± 8	10	3.0E–04
	20–30	0	0	0	0	29 ± 3	10	0	0	0	0	71 ± 5	10	3.7E–04
	30–40	5 ± 5	3	0	0	28 ± 6	10	0	0	0	0	67 ± 11	10	1.3E–03
	40–50	8 ± 0	6	0	0	35 ± 5	10	0	0	0	0	57 ± 11	10	9.9E–04
	50–60	17 ± 4	10	0	0	20 ± 2	10	2 ± 3	2	0	0	61 ± 1	10	1.2E–03
	60–70	8 ± 2	2	0	0	30 ± 0	10	0	0	0	0	62 ± 8	10	1.0E–03
	70–80	22 ± 3	3	0	0	8 ± 2	5	0	0	0	0	70 ± 13	10	1.2E–03
	80–90	25 ± 4	10	0	0	0	0	6 ± 3	2	0	0	69 ± 13	0	1.4E–03
	90–100	14 ± 6	8	0	0	9 ± 5	3	0	0	66 ± 4	10	12 ± 3	10	4.3E–03
H2	0–20	8 ± 0	2	0	0	14 ± 1	10	0	0	0	0	78 ± 5	10	2.6E–04
	20–30	10 ± 0	2	0	0	19 ± 1	10	0	0	0	0	72 ± 3	10	7.3E–04
	30–40	4 ± 6	2	0	0	27 ± 6	10	0	0	0	0	69 ± 12	10	1.3E–03
	40–50	26 ± 4	3	0	0	14 ± 3	10	0	0	0	0	60 ± 13	10	4.3E–04
	50–60	0	0	0	0	33 ± 1	10	0	0	11 ± 2	7	56 ± 12	10	9.4E–04
	60–70	0	0	0	0	32 ± 1	9	0	0	11 ± 1	7	57 ± 5	10	7.7E–04
	70–80	0	0	0	0	37 ± 1	10	0	0	17 ± 2	10	46 ± 6	10	1.1E–03
	80–90	0	3	9 ± 1	3	20 ± 1	7	0	0	58 ± 2	10	13 ± 1	0	1.0E–03

[a]Relative contributions of phosphorus forms in the best fit, *i.e.*, with the lowest assigned *R* values. Error estimates (±) refer to statistical uncertainty (*Ravel*, 2009) and do not consider uncertainties regarding data collection and treatment prior to LCF analysis.
[b]Number of occurrences of reference spectra representing a P group in the 10 best fits, *i.e.*, assigned the 10 lowest *R* values.
[c]Indicator value for goodness of fit, calculated according *Ravel* and *Newville* (2005).

even though the selectivity of pyrophosphate for soil organically complexed Al has been questioned (*Kaiser* and *Zech*, 1996). As was the case for Fe, Al-ox content exceeded Al-dith content consistently in the two profiles. However, the dithionite-extractable fraction of Al is less well-defined (*McKeague* et al., 1971)

4.2 Phosphorus speciation

The elevated top soil P content in in the two profiles was in agreement with results from previous studies (*Schlichting*, 2004; *Kruse* and *Leinweber*, 2008). Such P enrichment in cultivated Histosols has been attributed to P fertilisation (*Kaila* and *Missilä*, 1956; *Sundström* et al., 2000). For mineral soils, fertiliser-related P enrichment over time is well known (*Silveira* et al., 2006; *Annaheim* et al., 2015; *Schmieder* et al., 2018). However, in contrast to findings for cultivated mineral soils (*Silveira* et al., 2006; *Annaheim* et al., 2015), topsoil P speciation in both soils, according to LCF, was dominated by organic P. The results obtained with the ignition method were in direct contrast to this, as P-org-ig content increased with soil depth. However, we deem the LCF results to be more realistic. The vertical distribution of P-org in the LCF results for both soils was visibly corroborated by spectral features of the sample spectra. Furthermore, there were significant correlations between LCF results for mineral P and extractable Fe and Al in the profiles, supporting the P speciation and hence the distribution of P-org according to LCF. Ignition method results were not supported by complementary analysis.

Inaccuracies with the ignition method have previously been documented (*Williams* et al., 1970; *Turner* et al., 2005). Possible mechanisms of an overestimation of P-org include hydrolysis of organic P during acid extraction and/or incomplete extraction of P released during ignition (*Turner* et al., 2005).

Increasing P-org content in topsoil of cultivated Histosols has been observed in previous studies and attributed to accumulation of crop residues and inorganic P uptake in soil microbial biomass (*Kaila* and *Missilä*, 1956; *Schlichting*, 2004; *Pizzeghello* et al., 2014). Such accumulation of P-org requires that these processes are not compensated for by microbial P-org mineralisation, as is commonly the case in mineral soils. High C:P-org ratio in H1 and H2, amounting to1000 in the topsoil, indicated that microbial net P-org mineralisation is indeed very low in these soils.

Substrate nutrient stoichiometry in relation to decomposer biomass is an important indicator of organic matter decomposition and nutrient mineralisation (*Bosatta* and *Berendse*, 1984). Net P mineralisation should not occur unless the substrate C:P ratio falls below a critical ratio determined predominantly by the decomposer biomass stoichiometry (*Mooshammer* et al., 2012; *Spohn*, 2016). Despite high taxonomic diversity, the C:P ratio in soil microorganisms has been found to be well restrained at around 60 (*Richardson* and *Marshall*, 1986; *Cleveland* and *Liptzin*, 2007; *Spohn*, 2016). Significant net mineralisation of P-org in the H1 and H2 profiles is hence unlikely, since topsoil C:P ratios exceeded this ratio by a factor of 15. Microbial decomposition of substrate with unfavourable nutrient stoichiometry requires a reduction in decomposer carbon use efficiency, leading to a relative increase in mineralisation of organic carbon (*Manzoni* et al., 2010; *Sinsabaugh* et al., 2013). Hence, the substrate C:P ratio decreases with time until it approaches the critical C:P ratio allowing for net P mineralisation. This is probably reflected in the decrease in C:P ratio towards the topsoil of both profiles.

Average subsidence rate for Nordic peat soil is reported to be around 20 mm per year (*Stephens* et al., 1984). The time span of 70 years since drainage of the two profiles would hence correspond to a peat loss of more than 1 m. Much of the observed P accumulation would therefore be attributable to this soil subsidence. Transformation of inorganic fertiliser P into the organic P pool, as proposed by *Kaila* and *Missilä* (1956), could also have contributed to the observed P-org accumulation in the profiles. *Qualls* and *Richardson* (2000) report that topsoil microbial biomass increases up to nine-fold in Everglades's peat soils upon P fertilisation.

Throughout both profiles, P-org was represented by a lecithin reference and soil organic P reference spectra obtained for a peat soil horizon with extremely low ash content. However, the general potential of XANES LCF for organic P speciation is limited by the lack of specific spectral features in the XANES spectra of many organic P compounds (*Kruse* and *Leinweber*, 2008; see also Fig. 1). Generally, phytic acid has been found to be the predominant organic P form in soils, which is explained by its tendency to strongly bind to solid surfaces (*Gerke*, 2015).

Problems with a distinction between Al- and Fe-associated P based on XANES data have been reported previously (*Beauchemin* et al., 2003). The pre-edge shoulder, indicative of Fe–P, tends to be less pronounced in spectra of adsorbed forms of Fe–P than in those of Fe-phosphates (*Hesterberg* et al., 1999). Hence, in spectra of samples with relatively low concentrations of adsorbed Fe–P, identification and quantification of Fe–P is difficult, as post-edge oscillations are similar in spectra of both groups (Fig. 1). This may be further complicated by the energy shift in spectra of samples rich in P-org, such as the peat samples in this study, since the shifted absorption edge may superimpose part of the pre-edge shoulder.

However, while LCF weights and calculated contents of Fe–P were not meaningfully correlated with extractable Fe, pooling LCF results for Fe–P and Al–P increased the significance of the correlation with extractable Al. These observations could suggest a dominance of Al associated P over Fe–P in the profiles. In case of H1 this would be also supported by a considerably greater content of surface reactive Al in comparison with Fe-ox content.

Results from LCF in comparison with post-edge LCF for the organic soils could indicate the presence of P species that were not represented in the standard library. A hypothetical reference spectrum combining post edge features similar to mineral P spectra with an absorption edge shifted towards lower energy, typical for P-org species, could theoretically improve LCF performance for the sample spectra in question.

Phosphorus species that could reasonably be expected in organic soils and of which specific reference spectra were not included in the standard library are organic P forms associated with Fe or Al mineral surfaces. Phytate, the presumably most abundant form of organic P in soils is known to bind strongly to mineral surfaces (*Gerke*, 2015; *Prietzel* et al., 2016).

Prietzel et al. (2016) compared XANES spectra of phytate adsorbed to different Al and Fe mineral surfaces and Al and Fe saturated organic matter with spectra collected for orthophosphate adsorbed to the corresponding minerals. Particularly a spectrum for phytate sorbed to Al saturated organic matter featured indeed an absorption edge being slightly shifted towards lower energy in comparison with its orthophosphate counterpart, while at the same time featuring a similarly shaped post edge oscillation. A spectrum with such characteristics could have theoretically improved the fitting quality for sample spectra in which discrepancies between fit and sample in the post-edge region occurred. Even though there is no conclusive evidence, the presence of associations between P-org and mineral phases seems probable in these minerogenous fen peat soils. According to *Prietzel* and *Klysubun* (2018), spectra of phytate adsorbed to goethite tend to feature a clearly less pronounced pre-edge shoulder than corresponding orthophosphate spectra. Hence, the presence of such P species could also explain the lack of a correlation between Fe–P according to LCF and extractable Fe. The contribution of Fe–P could be expected to be underestimated by LCF if such spectra are not included in the reference library (*Prietzel* and *Klysubun*, 2018).

Self-absorption is known to limit the potential of soft XAS data obtained in fluorescence mode for quantitative P speciation. Using an approach devised by *Tröger* et al. (1992), *Hesterberg* et al. (1999) calculated self-absorption effects in mineral P samples of 800 mmol kg^{-1} to be around 8%, which was deemed acceptable for P speciation in soils samples. Standard P compounds in this thesis were prepared with the criterion of keeping the P concentration below 800 mmol kg^{-1}. If necessary, the samples were diluted using boron nitride, as widely done in previous studies (*Kelly* et al., 2008; *Kruse* et al., 2015).

Phosphorus K-edge XANES is a direct non-destructive analytical method requiring minimal sample pre-treatment, hence uncertainty regarding a potential chemical alteration of P in the sample can widely be avoided. However, the interpretation of XANES data based on LCF analysis is associated with uncertainty inherent to this merely statistical approach (*Ajiboye* et al., 2007). *Ajiboye* et al. (2007) studied the performance of LCF for binary mixtures of P compounds and observed the highest relative error on fitting a binary mixture of Fe–P (75%) and Ca–P (15%). In the final fit, the Fe–P weight amounted to 90% instead of the actual Fe–P proportion of 75% in the standard mixture. The potential for such error needs to be considered even higher in soils samples, likely containing several unknown P species. *Ajiboye* et al. (2007) did also show that the error in LCF fits tended to be higher for compound mixtures containing high proportions of P species whose XANES spectra lack clearly distinguishable spectral features. The latter is particularly valid for P-org rich samples, due to the lack of unique spectral features in XANES spectra of many organic P forms (*Kruse* and *Leinweber*, 2008). Quantitative P speciation based on linear fitting of sample XANES spectra of peat soils needs thus to be complemented with data from additional analytical techniques as was done in the present study. The meaningful and strong correlation observed between results from XANES LCF and wet chemical extractions do strongly support that the P speciation obtained for the sample soils is reasonable and realistic.

4.3 Implications for leaching

The phosphate sorption capacity of organic soils is known to depend primarily on Al- and Fe-minerals accumulated during formation of peat bodies (*Miller*, 1979; *Giesler* et al., 2005). Presence of Al- and Fe-minerals in different layers of the H1 profile showed that assessment of the potential to retain P in cultivated Histosols should include subsoil layers, as proposed for mineral soils (*Andersson* et al., 2013). Despite similar Fe-ox and Al-ox content in the topsoil of both profiles, the risk of mobilised P reaching drainpipes is lower in H1 due to substantially increased content of Al-ox in subsoil horizons. The majority of leaching studies carried out on organic soil report that P in leachate is predominantly in inorganic form (*Miller*, 1979; *Reddy*, 1983).

For mineral soils, a PSI above 0.3 indicates a high risk of P leaching losses (*De Smet* et al., 1995). However, risk assessment for leaching developed using the PSI of mineral soils may not be applicable to soils with high organic matter content, such as Histosols. Some studies report that organic matter forms metal complexes acting as sorbents for P (*Bloom*, 1981; *Gerke*, 2015), whereas others report increased mobility of P in soils with increasing organic matter content (*Guppy* et al., 2005; *Antelo* et al., 2007; *Lindegren* and *Persson*, 2009). Possible mechanisms for increased P mobility through organic matter can be competition of low-molecular weight organic anions with P for sorption sites, a shift in charge of mineral surfaces due to sorbed organic matter, and formation of soluble Al- and Fe-complexes (*Guppy* et al., 2005; *Sundman* et al., 2016). The presence of sorption sites available for P in organic soils may hence be lower than in mineral soils, despite similar Fe-ox and Al-ox content. Accordingly, critical PSI values indicating a high risk for leaching can be lower for organic than mineral soils.

P loss from organic soils may not exclusively occur in form of dissolved P. *Missong* et al. (2018), for instance, found colloidal P leaching a significant contribution to P loss from organic matter rich forest top soils. Also a potential impact of soil structure on P loss form peat soils needs to be mentioned. Shrinkage dynamics after peat reclamation are known to promote the formation of vertical cracks in drained peat soils providing potential flow paths for preferential P transport in form of colloidal and particulate P (*Schwärzel* et al., 2002; *Jarvis*, 2007)

Ferric Fe associated P can be of special importance in wetland soils, due to redox sensitivity of Fe^{3+} minerals and P release when reduced to Fe^{2+}. Reductive dissolution of Fe^{3+}

is frequently proposed to explain high P mobilisation in restored wetlands (*Jensen* et al., 1998; *Zak* and *Gelbrecht*, 2007; *Kjaergaard* et al., 2012). Our study showed that that the greater proportion of P in the profiles was associated with Al according to LCF. However, the smaller portion of soil P associated with Fe^{3+} can be more reactive and therefore be of a higher relevance for P losses under reducing conditions.

5 Conclusions

Phosphorus P-K-edge XANES, in combination with complementary analysis, revealed a dominance of organic P forms in two cultivated and fertilised fen peat profiles. Organic P was also dominating in the topsoil of the two profiles, where P levels were clearly elevated in comparison with subsoil layers. This enrichment of P-org in the upper soil despite large applications of inorganic fertilizer P over time is probably partly the result of inorganic P being transformed by soil microbiota of crop residues into organic forms. Moreover, the high C:P ratio in topsoil peat material indicated that net mineralisation of P-org is low. Only a minor fraction of P was bound to Al and even less to Fe minerals. In the mineral layer below the peat, calcium phosphate was the dominant P fraction in both profiles.

An important finding related to leaching of inorganic P from these soils was the accumulation of mineral particles in the organic layers. Content of mineral particles providing sorption sites for inorganic P varied between profile layers and were explained by the formation history. However, more abundant organic anions in organic soils and competition between these ions and phosphate entails that the capacity of Al and Fe sites to retain P in organic soils is probably lower than in mineral soils.

Continued cultivation of drained peat soils leads to subsistence. Over time, the large pools of organic P in both profiles can be completely mineralised and the risk of P leaching from these soils can be similar to that of 'legacy P' from mineral soils. On the other hand, reversal of drainage and re-establishment of persistent anaerobic conditions may prevent subsistence, but could instead lead to reductive dissolution of Fe-associated P.

Considering the high heterogeneity of Histosols and possible accumulation of mineral particles in organic layers, leaching risks based on the two organic soils studied cannot be generalized.

References

Ajiboye, B., *Akinremi, O. O.*, *Jürgensen, A.* (2007): Experimental validation of quantitative XANES analysis for phosphorus speciation. *Soil. Sci. Soc. Am. J.* 71, 1288–1291.

Andersson, H., *Bergström, L.*, *Djodjic, F.*, *Ulén, B.*, *Kirchmann, H.* (2013): Topsoil and subsoil properties influence phosphorus leaching from four agricultural soils. *J. Environ. Qual.* 42, 455–463.

Annaheim, K. E., *Doolette, A. L.*, *Smernik, R. J.*, *Mayer, J.*, *Oberson, A.*, *Frossard, E.*, *Bünemann, E. K.* (2015): Long-term addition of organic fertilizers has little effect on soil organic phosphorus as characterized by ^{31}P NMR spectroscopy and enzyme additions. *Geoderma* 257, 67–77.

Antelo, J., *Arce, F.*, *Avena, M.*, *Fiol, S.*, *López, R.*, *Macías, F.* (2007): Adsorption of a soil humic acid at the surface of goethite and its competitive interaction with phosphate. *Geoderma* 138, 12–19.

Beauchemin, S., *Hesterberg, D.*, *Chou, J.*, *Beauchemin, M.*, *Simard, R. R.*, *Sayers, D. E.* (2003): Speciation of phosphorus in phosphorus-enriched agricultural soils using X-ray absorption near-edge structure spectroscopy and chemical fractionation. *J. Environ. Qual.* 32, 1809–1819.

Bedrock, C. N., *Cheshire, M. V.*, *Chudek, J. A.*, *Goodman, B. A.*, *Shand, C. A.* (1994): Use of ^{31}P-NMR to study the forms of phosphorus in peat soils. *Sci. Total. Environ.* 152, 1–8.

Berglund, Ö., *Berglund, K.* (2010): Distribution and cultivation intensity of agricultural peat and gyttja soils in Sweden and estimation of greenhouse gas emissions from cultivated peat soils. *Geoderma* 154, 173–180.

Biester, H., *Knorr, K. H.*, *Schellekens, J.*, *Basler, A.*, *Hermanns, Y. M.* (2014): Comparison of different methods to determine the degree of peat decomposition in peat bogs. *Biogeosciences* 11, 2691–2707.

Bloom, P. R. (1981): Phosphorus adsorption by an aluminium–peat complex. *Soil Sci. Soc. Am. J.* 45, 267–272.

Bosatta, E., *Berendse, F.* (1984): Energy or nutrient regulation of decomposition: Implications for the mineralization-immobilization response to perturbations. *Soil. Biol. Biochem.* 16, 63–67.

Cleveland, C. C., *Liptzin, D.* (2007): C:N:P stoichiometry in soil: is there a "Redfield ratio" for the microbial biomass? *Biogeochemistry* 85, 235–252.

Condron, L. M., *Newman, S.* (2011): Revisiting the fundamentals of phosphorus fractionation of sediments and soils. *J. Soil. Sediment.* 11, 830–840.

De Smet, J., *Hofman, G.*, *Vanderdeelen, J.*, *Van Meirvenne, M.*, *Baert, L.* (1995): Phosphate enrichment in the sandy loam soils of West-Flanders, Belgium. *Fertil. Res.* 43, 209–215.

Drzymulska, D. (2016): Peat decomposition—shaping factors, significance in environmental studies and methods of determination; a literature review. *Geologos* 22, 61–69.

Duxbury, J. M., *Peverly, J. H.* (1978): Nitrogen and phosphorus losses from organic soils. *J. Environ. Qual.* 7, 566–570.

Emsens, W. J., *Aggenbach, C. J. S.*, *Schoutens, K.*, *Smolders, A. J. P.*, *Zak, D.*, *van Diggelen, R.* (2016): Soil iron content as a predictor of carbon and nutrient mobilization in rewetted fens. *PLoS One* 11. DOI: https://doi.org/10.1371/journal.pone.0153166.

Eriksson, A. K., *Hesterberg, D.*, *Klysubun, W.*, *Gustafsson, J. P.* (2016): Phosphorus dynamics in Swedish agricultural soils as influenced by fertilization and mineralogical properties: insights gained from batch experiments and XANES spectroscopy. *Sci. Total Environ.* 566, 1410–1419.

Eveborn, D., *Gustafsson, J. P.*, *Elmefors, E.*, *Yu, L.*, *Eriksson, A. K.*, *Ljung, E.*, *Renman, G.* (2014): Phosphorus in soil treatment systems: accumulation and mobility. *Water Res.* 64, 42–52.

Eveborn, D., *Gustafsson, J. P.*, *Hesterberg, D.*, *Hillier, S.* (2009): XANES speciation of P in environmental samples: An assessment of filter media for on-site wastewater treatment. *Environ. Sci. Technol.* 43, 6515–6521.

Gerke, J. (2015): Phytate (inositol hexakisphosphate) in soil and phosphate acquisition from inositol phosphates by higher plants. A review. *Plants* 4, 253–266.

Giesler, R., *Andersson, T.*, *Lövgren, L.*, *Persson, P.* (2005): Phosphate sorption in aluminum-and iron-rich humus soils. *Soil Sci. Soc. Am. J.* 69, 77–86.

Guppy, C. N., *Menzies, N. W.*, *Moody, P. W.*, *Blamey, F. P. C.* (2005): Competitive sorption reactions between phosphorus and organic matter in soil: a review. *Soil Res.* 43, 189–202.

Hedley, M. J., *Stewart, J. W. B.*, *Chauhan, B. S.* (1982): Changes in inorganic and organic soil phosphorus fractions induced by cultivation practices and by laboratory incubations. *Soil. Sci. Soc. Am. J.* 46, 970–976.

Hesterberg, D. (2010): Macroscale Chemical Properties and X-Ray Absorption Spectroscopy of Soil Phosphorus, in Singh, B., Gräfe, M. (eds.): Developments in Soil Science, Synchrotron-Based Techniques in Soils and Sediments. Elsevier, Amsterdam, The Netherlands, pp. 313–356.

Hesterberg, D., *Zhou, W.*, *Hutchison, K. J.*, *Beauchemin, S.*, *Sayers, D. E.* (1999): XAFS study of adsorbed and mineral forms of phosphate. *J. Synchrotron Radiat.* 6, 636–638.

Hill, B. M., *Siegel, D. I.* (1991): Groundwater flow and the metal content of peat. *J. Hydrol.* 123, 211–224.

Holmgren, G. G. S. (1967): A rapid citrate-dithionite extractable iron procedure. *Soil. Sci. Soc. Am. J.* 31, 210–211.

ISO 11074 (2015): Soil Quality—Vocabulary. Beuth, Berlin, Germany.

ISO 11277 (2009): Soil Quality—Determination of Particle Size Distribution in Mineral Soil Material: Method by Sieving and Sedimentation. Beuth, Berlin, Germany.

ISO 11885 (2007): Water Quality—Determination of Selected Elements by Inductively Coupled Plasma Optical Emission Spectrometry (ICP-OES). Beuth, Berlin, Germany.

ISO 13878 (1998): Soil Quality—Determination of Total Nitrogen Content by Dry Combustion ("Elemental Analysis"). Beuth, Berlin, Germany.

Jarvis, N. J. (2007): A review of non-equilibrium water flow and solute transport in soil macropores: principles, controlling factors and consequences for water quality. *Eur. J. Soil. Sci.* 58, 523–546.

Jensen, M. B., *Hansen, H. C. B.*, *Nielsen, N. E.*, *Magid, J.* (1998): Phosphate mobilization and immobilization in two soils incubated under simulated reducing conditions. *Acta Agric. Scand. B Soil Plant Sci.* 48, 11–17.

Kaila, A., *Missilä, H.* (1956): Accumulation of fertilizer phosphorus in peat soils. *Agric. Food Sci.* 28, 168–178.

Kaiser, K., *Zech, W.* (1996): Defects in estimation of aluminum in humus complexes of podzolic soils by pyrophosphate extraction. *Soil Sci.* 161, 452–458.

Kasimir-Klemedtsson, Å., *Klemedtsson, L.*, *Berglund, K.*, *Martikainen, P.*, *Silvola, J.*, *Oenema, O.* (1997): Green-house gas emissions from farmed organic soils: a review. *Soil Use Manage.* 13, 245–250.

Kelly, S. D., *Hesterberg, D.*, *Ravel, B.* (2008): Analysis of Soils and Minerals using X-ray Absorption Spectroscopy, in Ulery, A. L., Drees, L. R. (eds.): Methods of Soil Analysis, Part 5, Mineralogical Methods. SSSA, Madison, WI, USA, pp. 387–463.

Kizewski, F., *Liu, Y. T.*, *Morris, A.*, *Hesterberg, D.* (2011): Spectroscopic approaches for phosphorus speciation in soils and other environmental systems. *J. Environ. Qual.* 40, 751–766.

Kjaergaard, C., *Heiberg, L.*, *Jensen, H. S.*, *Hansen, H. C. B.* (2012): Phosphorus mobilization in rewetted peat and sand at variable flow rate and redox regimes. *Geoderma* 173, 311–321.

Klysubun, W., *Sombunchoo, P.*, *Deenan, W.*, *Kongmark, C.* (2012): Performance and status of beamline BL8 at SLRI for X-ray absorption spectroscopy. *J. Synchrotron Radiat.* 19, 930–936.

Knox, S. H., *Sturtevant, C.*, *Matthes, J. H.*, *Koteen, L.*, *Verfaillie, J.*, *Baldocchi, D.* (2015): Agricultural peatland restoration: effects of land-use change on greenhouse gas (CO_2 and CH_4) fluxes in the Sacramento-San Joaquin Delta. *Global Change Biol.* 21, 750–765.

Kruse, J., *Abraham, M.*, *Amelung, W.*, *Baum, C.*, *Bol, R.*, *Kühn, O.*, *Lewandowski, H.*, *Niederberger, J.*, *Oelmann, Y.*, *Rüger, C.*, *Santner, J.*, *Siebers, M.*, *Siebers, N.*, *Spohn, M.*, *Vestergren, J.*, *Vogts, A.*, *Leinweber, P.* (2015): Innovative methods in soil phosphorus research: A review. *J. Plant. Nutr. Soil Sci.* 178, 43–88.

Kruse, J., *Leinweber, P.* (2008): Phosphorus in sequentially extracted fen peat soils: A K-edge X-ray absorp-tion near-edge structure (XANES) spectroscopy study. *J. Plant Nutr. Soil Sci.* 171, 613–620.

Kuo, S. (1996): Phosphorus, in Sparks, D. L. (ed.): Methods of Soil Analysis, Part 3, Chemical Methods. SSSA, Madison, WI, USA, pp. 869–920.

Leifeld, J., *Müller, M.*, *Fuhrer, J.* (2011): Peatland subsidence and carbon loss from drained temperate fens. *Soil Use Manage.* 27, 170–176.

Li, M., *Zhang, J.*, *Wang, G.*, *Yang, H.*, *Whelan, M. J.*, *White, S. M.* (2013): Organic phosphorus fractionation in wetland soil profiles by chemical extraction and phosphorus-31 nuclear magnetic resonance spectroscopy. *Appl. Geochem.* 33, 213–221.

Lindegren, M., *Persson, P.* (2009): Competitive adsorption between phosphate and carboxylic acids: quantitative effects and molecular mechanisms. *Eur. J. Soil. Sci.* 60, 982–993.

Longabucco, P., *Rafferty, M. R.* (1989): Delivery of nonpoint-source phosphorus from cultivated mucklands to Lake Ontario. *J. Environ. Qual.* 18, 157–163.

Lookman, R., *Jansen, K.*, *Merckx, R.*, *Vlassak, K.* (1995): Geostatistical assessment of the regional distribution of phosphate sorption capacity parameters (Fe_{ox} and Al_{ox}) in northern Belgium. *Geoderma* 66, 285–296.

Manzoni, S., *Trofymow, J. A.*, *Jackson, R. B.*, *Porporato, A.* (2010): Stoichiometric controls on carbon, nitrogen, and phosphorus dynamics in decomposing litter. *Ecol. Monogr.* 80, 89–106.

McCray, J. M., *Wright, A. L.*, *Luo, Y.*, *Ji, S.* (2012): Soil phosphorus forms related to extractable phosphorus in the everglades agricultural area. *Soil Sci.* 177, 31–38.

McKeague, J. A. (1967): An evaluation of 0.1M pyrophosphate and pyrophosphate–dithionite in comparison with oxalate as extractants of the accumulation products in Podzols and some other soils. *Can. J. Soil Sci.* 47, 95–99.

McKeague, J. A., *Brydon, J. E.*, *Miles, N. M.* (1971): Differentiation of forms of extractable iron and aluminum in soils. *Soil Sci. Soc. Am. J.* 35, 33–38.

Mehra, O. P., *Jackson, M. L.* (1960): Iron Oxide Removal from Soils and Clay by a Dithionite-Citrate System Buffered with Sodium Bicarbonate, in Ingerson, E. (ed.): Clays and Clay Minerals. Pergamon Press, Oxford, UK, pp. 317–327.

Miller, M. H. (1979): Contribution of nitrogen and phosphorus to subsurface drainage water from intensively cropped mineral and organic soils in Ontario. *J. Environ. Qual.* 8, 42–48.

Missong, A., *Bol, R.*, *Nischwitz, V.*, *Krüger, J.*, *Lang, F.*, *Siemens, J.*, *Klumpp, E.* (2018): Phosphorus in water dispersible-colloids of forest soil profiles. *Plant Soil* 427, 71–86.

Mooshammer, M., *Wanek, W.*, *Schnecker, J.*, *Wild, B.*, *Leitner, S.*, *Hofhansl, F.*, *Blöchl, A.*, *Hämmerle, I.*, *Frank, A. H.*, *Fuchslueger, L.*, *Keiblinger, K. M.*, *Zechmeister-Boltenstern, S.*, *Richter, A.* (2012): Stoichiometric controls of nitrogen and phosphorus cycling in decomposing beech leaf litter. *Ecology* 93, 770–782.

Oenema, O. (1990): Pyrite accumulation in salt marshes in the Eastern Scheldt, southwest Netherlands. *Biogeochemistry* 9, 75–98.

Oleszczuk, R., *Regina, K.*, *Szajdak, L.*, *Höper, H.*, *Maryganova, V.* (2008): Impacts of Agricultural Utilization of Peat Soils on the Greenhouse Gas Balance, in Strack, M. (ed.): Peatlands and Climate Change. International Peat Society, Jyväskylä, Finland, pp. 70–97.

Pizzeghello, D., *Berti, A.*, *Nardi, S.*, *Morari, F.* (2014): Phosphorus-related properties in the profiles of three Italian soils after long-term mineral and manure applications. *Agric. Ecosyst. Environ.* 189, 216–228.

Prietzel, J., *Thieme, J.*, *Paterson, D.* (2010): Phosphorus speciation of forest-soil organic surface layers using P K-edge XANES spectroscopy. *J. Plant. Nutr. Soil Sci.* 173, 805–807.

Prietzel, J., *Harrington, G.*, *Häusler, W.*, *Heister, K.*, *Werner, F.*, *Klysubun, W.* (2016): Reference spectra of important adsorbed organic and inorganic phosphate binding forms for soil P speciation using synchrotron-based K-edge XANES spectroscopy. *J. Synchrotron Radiat.* 23, 532–544.

Prietzel, J., *Klysubun, W.* (2018): Phosphorus K-edge XANES spectroscopy has probably often underestimated iron oxyhydroxide-bound P in soils. *J. Synchrotron Radiat.* 25, 1736–1744.

Qualls, R. G., *Richardson, C. J.* (2000): Phosphorus enrichment affects litter decomposition, immobilization, and soil microbial phosphorus in wetland mesocosms. *Soil. Sci. Soc. Am. J.* 64, 799–808.

Ravel, B. (2009): Athena: A User's Guide. Available at: http://bruceravel.github.io/demeter/aug/ (last accessed February 17, 2017).

Ravel, B., *Newville, M.* (2005): ATHENA, ARTEMIS, HEPHAESTUS: Data analysis for X-ray absorption spectroscopy using IFEFFIT. *J. Synchrotron Radiat.* 12, 537–541.

Reddy, K. R. (1983): Soluble phosphorus release from organic soils. *Agric. Ecosyst. Environ.* 9, 373–382.

Richardson, C. J., *Marshall, P. E.* (1986): Processes controlling movement, storage, and export of phosphorus in a fen peatland. *Ecol. Monogr.* 56, 279–302.

Robinson, J. S., *Johnston, C. T.*, *Reddy, K. R.* (1998): Combined chemical and ^{31}P-NMR spectroscopic analysis of phosphorus in wetland organic soils. *Soil Sci.* 163, 705–713.

Schindler, D. W. (1977): Evolution of phosphorus limitation in lakes. *Science* 195, 260–262.

Schlichting, A. (2004): Phosphorstatus und -umsetzungen in degradierten und wiedervernässten Niedermooren. PhD thesis, University of Rostock, Germany.

Schmieder, F., *Bergström, L.*, *Riddle, M.*, *Gustafsson, J. P.*, *Klysubun, W.*, *Zehetner, F.*, *Condron, L.*, *Kirchmann, H.* (2018): Phosphorus speciation in a long-term manure-amended soil profile—Evidence from wet chemical extraction, ^{31}P-NMR and P K-edge XANES spectroscopy. *Geoderma* 322, 19–27.

Schwertmann, U. (1964): Differenzierung der Eisenoxide des Bodens durch Extraktion mit Ammoniumoxalat-Lösung. *Z. Pflanz. Dueng. Bodenkunde* 105, 194–202.

Schwärzel, K., *Renger, M.*, *Sauerbrey, R.*, *Wessolek, G.* (2002): Soil physical characteristics of peat soils. *J. Plant Nutr. Soil Sci.* 165, 479–486.

Silveira, M. L., *Miyittah, M. K.*, *O'Connor, G. A.* (2006): Phosphorus release from a manure-impacted spodosol: effects of a water treatment residual. *J. Environ. Qual.* 35, 529–541.

Sinsabaugh, R. L., *Manzoni, S.*, *Moorhead, D. L.*, *Richter, A.* (2013): Carbon use efficiency of microbial communities: stoichiometry, methodology and modelling. *Ecol. Lett.* 16, 930–939.

Smieja-Król, B., *Fiałkiewicz-Kozieł, B.* (2014): Quantitative determination of minerals and anthropogenic particles in some Polish peat occurrences using a novel SEM point-counting method. *Environ. Monit. Assess.* 186, 2573–2587.

Spohn, M. (2016): Element cycling as driven by stoichiometric homeostasis of soil microorganisms. *Basic Appl. Ecol.* 17, 471–478.

Steinmann, P., *Shotyk, W.* (1997): Geochemistry, mineralogy, and geochemical mass balance on major elements in two peat bog profiles (Jura Mountains, Switzerland). *Chem. Geol.* 138, 25–53.

Stephens, J. C., *Allen, L. H.*, *Chen, E.* (1984): Organic soil subsidence. *Rev. Eng. Geol.* 6, 107–122.

Stoppe, N., *Amelung, W.*, *Horn, R.* (2015): Chemical extraction of sedimentary iron oxy(hydr)oxides using ammonium oxalate and sodium dithionite revisited—an explanation of processes in coastal sediments. *Agro Sur* 43, 11–17.

Sundman, A., *Karlsson, T.*, *Sjöberg, S.*, *Persson, P.* (2016): Impact of iron–organic matter complexes on aqueous phosphate concentrations. *Chem. Geol.* 426, 109–117.

Sundström, E., *Magnusson, T.*, *Hånell, B.* (2000): Nutrient conditions in drained peatlands along a north-south climatic gradient in Sweden. *Forest Ecol. Manage.* 126, 149–161.

Tannazi, F., *Bunker, G.* (2005): Determination of chemical speciation by XAFS. *Phys. Scripta* 2005. DOI: https://doi.org/10.1238/Physica.Topical.115a00953.

Tolonen, K. (1984): Interpretation of changes in the ash content of ombrotrophic peat layers. *Bull. Geol. Soc. Finland.* 56, 207–219.

Tröger, L., *Arvanitis, D.*, *Baberschke, K.*, *Michaelis, H.*, *Grimm, U.*, *Zschech, E.* (1992): Full correction of the self-absorption in soft-fluorescence extended x-ray-absorption fine structure. *Phys. Rev. B* 46, 3283–3289.

Turner, B. L., *Cade-Menun, B. J.*, *Condron, L. M.*, *Newman, S.* (2005): Extraction of soil organic phosphorus. *Talanta* 66, 294–306.

Ulén, B., *Jakobsson, C.* (2005): Critical evaluation of measures to mitigate phosphorus losses from agricultural land to surface waters in Sweden. *Sci. Total Environ.* 344, 37–50.

Williams, J. D. H., *Syers, J. K.*, *Walker, T. W.*, *Rex, R. W.* (1970): A comparison of methods for the determination of soil organic phosphorus. *Soil Sci.* 110, 13–18.

Zak, D., *Gelbrecht, J.* (2007): The mobilization of phosphorus, organic carbon and ammonium in the initial stage of fen rewetting (a case study from NE Germany). *Biogeochemistry* 85, 141–151.

Zak, D., *Wagner, C.*, *Payer, B.*, *Augustin, J.*, *Gelbrecht, J.* (2010): Phosphorus mobilization in rewetted fens: the effect of altered peat properties and implications for their restoration. *Ecol. Appl.* 20, 1336–1349.

Zuo, M., *Renman, G.*, *Gustafsson, J. P.*, *Renman, A.* (2015): Phosphorus removal performance and speciation in virgin and modified argon oxygen decarburisation slag designed for wastewater treatment. *Water Res.* 87, 271–281.